

See discussions, stats, and author profiles for this publication at:
<https://www.researchgate.net/publication/263126566>

Nanofibrillated cellulose originated from birch sawdust after sequential extractions: A promising polymeric material from waste to films

ARTICLE *in* CELLULOSE · JUNE 2014

Impact Factor: 3.57 · DOI: 10.1007/s10570-014-0321-4

CITATIONS

8

READS

80

5 AUTHORS, INCLUDING:



Risto I. Korpinen

Natural Resources Institute Finland (L...

15 PUBLICATIONS 32 CITATIONS

SEE PROFILE



Kirsi S. Mikkonen

University of Helsinki

34 PUBLICATIONS 472 CITATIONS

SEE PROFILE



Stefan M Willför

Åbo Akademi University

168 PUBLICATIONS 3,107 CITATIONS

SEE PROFILE



Chunlin Xu

Åbo Akademi University

50 PUBLICATIONS 463 CITATIONS

SEE PROFILE

Nanofibrillated cellulose originated from birch sawdust after sequential extractions: a promising polymeric material from waste to films

Jun Liu · Risto Korpinen · Kirsi S. Mikkonen · Stefan Willför · Chunlin Xu

Received: 7 June 2013 / Accepted: 4 June 2014
© Springer Science+Business Media Dordrecht 2014

Abstract The residual cellulose of wood processing waste, sawdust, which was leftover after sequential hot-water extraction processes to isolate hemicelluloses and lignin in a novel forest biorefinery concept, was explored as the starting material for preparation of a highly value-added polymeric material, nanofibrillated cellulose (NFC) also widely termed as cellulose nanofiber, which has provided an alternative efficient way to upgrade sawdust waste. The residual cellulose in sawdust was converted to a transparent NFC suspension in water through the 2,2,6,6-tetramethylpiperidine-1-oxyl/NaClO/NaBr oxidation approach. The resultant NFC with a dimension of ca. 5 nm in width and hundreds of nanometers in length were further processed into NFC films. The

morphological features of the NFC suspension and its films were assessed by transmission electron microscopy and scanning electron microscopy. Highly even dispersion of NFC fibrils in the films originated from sawdust feasibly contributes to the outstanding mechanical performance of the films. NFC suspension with higher carboxylate content and its resultant NFC films were found to show higher transmission of light.

Keywords Nanofibrillated cellulose · Cellulose nanofiber · Sawdust · TEMPO oxidation · Biorefinery

Introduction

Utilization of biomass for production of various high value products such as biocomposites, particularly under the concept of ‘biorefinery’, has recently attracted a lot of attention owing to its environmentally friendly properties relative to petro-based synthetic materials (FitzPatrick et al. 2010). However, great challenges (e.g., a lack of innovative approaches to preserve the sophisticated structure and chemical natures of the biomass so as to develop high-value products) are limiting technology development and the process feasibility of biorefineries. We have been developing an approach in which each component of wood material is sequentially extracted with its unique structure preserved for further tailoring into functional materials (Borrega et al. 2012; Song et al. 2011).

Electronic supplementary material The online version of this article (doi:10.1007/s10570-014-0321-4) contains supplementary material, which is available to authorized users.

J. Liu · R. Korpinen · S. Willför · C. Xu (✉)
Process Chemistry Centre, c/o Laboratory Wood and
Paper Chemistry, Åbo Akademi University, Porthansgatan
3, 20500 Åbo/Turku, Finland
e-mail: chunlin.xu@abo.fi; cxu@abo.fi

K. S. Mikkonen
Department of Food and Environmental Sciences,
University of Helsinki, P.O. Box 27, 00014 Helsinki,
Finland

C. Xu
Wallenberg Wood Science Center, KTH The Royal
Institute of Technology, 10044 Stockholm, Sweden

Sawdust or wood dust is a by-product when timber or wood materials are processed, for instance when they are chipped, sawed, turned, drilled or sanded. Industries such as sawmills, dimension mills, furniture manufactures, cabinetmaking and carpentry are the main producers of sawdust. Total round wood production and total sawn wood production in EU countries were 428 and 103 million cubic meters in 2010, respectively (Eurostat 2013). Traditionally, sawdust is used to prepare charcoal, as an absorbent for nitroglycerin or effluents containing heavy metals, as filler in plastics, as wood composts and in linoleum and paperboard (Weber et al. 1993). However, flammability and other potential hazards which undermine workers' health hinder the full utilization of sawdust (Blot 1997; Demers et al. 1995). For example, Tatrai et al. (1995) identified cellulose in pine wood dust as the agent responsible for pulmonary inflammation and fibrosis, while cellulose is one of the most important components in many biorefinery concepts. Therefore, exploration of high value-added products from this controversial raw material will definitely extend the concept of biorefinery.

Exploration and utilization of cellulose in the concept of a novel biorefinery has attracted increasing attention in recent decades due to its abundance in nature, biodegradability and renewability (Ohara 2003). Recently, much research has focused on tailoring cellulose into nanostructured composites or nanopapers (Abdul Khalil et al. 2012). For nano-scale cellulose fibers, such as nanofibrillated cellulose (NFC), the surface charge, surface energy, specific area, crystalline structure and size and some other properties are sometimes significantly different from those of the bulk materials, and thus offer promising application opportunities (Siqueira et al. 2010). NFC-based biocomposites are one group of the most promising research sub-areas. Apart from the advantages of being natural fibers, NFC-based composites also possess very high strength and stiffness, turning them into an excellent reinforcing agent for nanocomposites. In the current approach of treating sawdust as biomass, sequential extractions were applied to isolate the valuable components, lignin and hemicelluloses, instead of removing the water-soluble fraction by degradation, which not only consumes more chemicals, but also wastes the biomass (Okita et al. 2009). The lignin can be tailored for the manufacturing of fine

chemicals such as vanillin by oxidation or to produce carbon fiber, adhesives, resin etc. (Zakzeski et al. 2010). The fractionated hemicelluloses can be further developed for food additive, pharmaceutical and cosmetic applications or as a starting material for the production of functional polymers (Ebringerová et al. 2008). The cellulose residue in the present study was developed for the preparation of NFC.

Traditional mechanical approaches used to prepare NFC are limited due to their higher energy consumption and the low quality of the heterogeneous product. 2,2,6,6-tetramethylpiperidine-1-oxyl radical (TEMPO) mediated oxidation of native cellulose, a promising alternative approach, is a type of regioselective surface modification of crystalline native cellulose microfibrils, and allows the formation of anionic carboxylate groups with quite high densities on the microfibril surfaces (Saito et al. 2007). The aim of the present study was to demonstrate the feasibility of the TEMPO-mediated oxidation approach to prepare NFC from sequentially extracted wood waste—birch sawdust by hot-water extraction and soda cooking. Moreover, films were obtained from the NFC suspension and investigated for potential applications in advanced materials.

Materials and methods

Materials

Unbleached birch sawdust pulp after hot-water extraction and subsequent delignification was used as the starting material in the present study. The initial kappa number of the pulp was 4.7 and brightness 59.9 % ISO. A commercial bleached birch kraft pulp (BKP) with a brightness of 83.3 % was directly used as a reference to prepare NFC, and no further extraction pretreatments were conducted for the preparation of NFC.

Furthermore, TEMPO, sodium bromide, sodium hypochlorite solution (10 wt%), and other chemical products were purchased from Sigma Aldrich and used without further purification. Of the bleaching agents, chlorine dioxide solution (ClO₂ content 9.94 g/L) was obtained from a pulp mill and stored in a refrigerator. Finally, the H₂O₂ solution (30 wt%) was supplied by MERCK.

Pretreatment of extracted sawdust pulp

A four-stage elemental chlorine free (ECF) bleaching sequence (D0(EP)1D1(EP)2, where D stands for a chlorine dioxide stage, (EP) for an alkaline extraction with peroxide stage, and the numerical subscript means the stage of sequence bleaching, was used to bleach the sawdust pulp to reach a comparable value to that of the reference BKP. The main bleaching conditions used are presented in Table 1. After each bleaching stage, the pulps were washed with distilled water three times with a weight ratio of 1:20. The final brightness of the bleached sawdust pulp was 82.4 % ISO, close to that of the reference BKP (83.3 % ISO). Kappa number, intrinsic viscosity (η) and brightness of the pulp were measured according to SCAN-test standard procedures, and the average degree of polymerization (DP) of the pulps were calculated according to the formula of $DP^{0.90} = 1.65[\eta]$ (Evans and Wallis 1989). The resultant pulp was thereafter utilized for the preparation of NFC.

Determination of fiber morphology

Fiber morphology of the pulps was measured using a Kajaani FiberLab Analyzer. The measuring speed was approximately 90 fibers per second and the analysis consistency of the sample was 0.005–0.01 %.

TEMPO-mediated oxidation and mechanical fibrillation of cellulose

Procedures were optimized from Saito et al. (2007). Cellulose fibers (2 g) were dispersed in 100 mL

distilled water and stirred for 4.0 h at room temperature; 100 mL solution containing 32 mg TEMPO (0.1 mmol/g fiber) and 200 mg sodium bromide (1.0 mmol/g fiber) were mixed with the dispersed fiber suspension and the pH of the slurry was adjusted to 10.0 by the addition of 0.5 M NaOH. The oxidation was started by adding the desired amount of the 10 % NaClO dropwise (5–10 mmol/g fiber). The total volume of the NaClO was added within the one third of the designated reaction time and the pH was maintained at 10.5 by adding 0.5 M NaOH. The equilibrium of the reaction was assumed to reach until no NaOH consumption was observed. The TEMPO-oxidized cellulose was precipitated in ethanol with a ratio of 1:3 (v/v) and thoroughly washed with distilled water by filtration, and the residual ethanol was removed by rotary evaporation. The oxidized cellulose at a consistency of 0.5 % was fibrillated by a domestic blender (OBH Nordica 6658, Denmark) for 2 min at an output of 300 W and then stored at 4.0 °C before further analysis.

Preparation of TEMPO-oxidized cellulose films

The TEMPO-oxidized cellulose was diluted to 0.1 % (w/v) and the air was removed by vacuum suction. About 300 mL of the suspension was filtrated on a nylon membrane filter with 0.1 μ m pore size and 90 mm diameter (Sterlitech, USA). After drying in vacuum desiccator at 40 °C at a pressure of 88 mbar for 4.0 h, a film with a thickness of 45 ± 5 μ m, moisture content of ca. 20 % and yield of 92–97 % was obtained.

Determination of carboxylate content

Conductometric titration was applied to determine the carboxylate content; 50 mg of NFC was diluted to 0.1 % (w/v) and 2.0 mL of 0.1 M HCl was added to exchange the sodium ions bound to the carboxyl groups by protons. Then, 1.0 mL of 1.0 mM NaCl was added to promote the dynamic distribution equilibrium of the ions and the slurry was sufficiently stirred for 90 min before titration. When a stable suspension was obtained, the mixture was titrated with 0.1 M NaOH at the rate of 0.1 mL/min and the carboxylate content of the sample was calculated from the conductivity and pH curves, from where the strong acid corresponding to the excess added HCl and weak

Table 1 Bleaching sequences and conditions

Bleaching conditions	Bleaching stage			
	D ₀	(EP) ₁	D ₁	(EP) ₂
Consistency (%)	10	10	10	10
Temperature (°C)	60	70	60	70
Time (min)	90	120	90	120
Kappa factor	0.3	–	0.3	–
pH	3.5	11.8	3.5	11.8
ClO ₂ (kg/t)	1.41	–	1.41	–
H ₂ SO ₄ (kg/t)	2.5	–	2.5	–
H ₂ O ₂ (kg/t)	–	3.5	–	3.5
NaOH (kg/t)	–	5	–	5

D, chlorine dioxide; E, alkaline extraction; P, hydrogen peroxide

acid supposed to be the carboxyl group can be observed (Araki et al. 2001).

Transmission electron microscopy (TEM)

Drops of diluted NFC suspension in water (0.05 % w/v) were deposited on carbon-coated electron microscope grids, after which one drop of 2 % uranyl acetate negative stain was added and the sample was stained for 40 s. Excess solution was blotted out with a filter paper and the sample was allowed to stand for drying. The grids were observed with a Philips FEI TECNAI 12 TEM (FEI Company, Hillsboro, USA) operated at an accelerating voltage of 120 kV.

UV–Vis transmittance measurement

Transmittance spectra of the NFC suspension at a concentration of 0.1 % in the range of 300–1,000 nm were measured using a Perkin Elmer Lambda 40 UV/Vis spectrometer at a scan speed of 240 nm/min and slit of 2.0 nm. The films of NFC were also measured at the same condition (Supplementary Material Figure S1).

Optical microscopy (OM) and polarizing optical microscopy (P-OM)

Optical imaging of the films was taken using transmitted light with a ZEISS Axio Scope A1 polarizing optical microscope equipped with an AxioCam ICc3 camera (Carl ZEISS, Germany).

Scanning electron microscopy (SEM)

Morphology of NFC films' surface was observed using a LEO Gemini 1530 with a Thermo Scientific UltraDry Silicon Drift Detector (SDD) (LEO, Oberkochen, Germany). The nonconductive samples were coated with carbon prior to the measurements.

Mechanical properties of films

The tensile strength, elongation at break, and Young's modulus of the films with ca. 5 mm width were determined at 5 mm/min using an Instron universal testing machine [Instron-33R4465, (Instron Corp., High Wycombe, England)] equipped with a static load cell of 100 N and an initial grip distance of 20 mm.

Before the main run at 5 mm/min, a pre-run was done with the tensile tester at a rate of 2 mm/min until 0.1 N load was reached so as to eliminate the error that is caused by loosely attached samples. The mechanical testing was conducted at 23 °C and 50 % RH in a climate room. The thickness of the specimens was measured as an average of three points using a micrometer (Lorentzen & Wettre, Kista, Sweden, precision 1 µm), and width was measured with a digital caliper (Mahr GmbH 16ER, Germany, precision 10 µm). Ten specimens from three replicate films of each sample were tested after conditioning at 50 % RH and 23 °C.

Dynamic mechanical analysis (DMA) was carried out using a DMA 242 (Netzsch-Gerätebau GmbH, Selb, Germany) in tension mode. The storage modulus was recorded as a function of temperature from –100 to 130 °C at a heating rate of 5 °C/min, and a frequency of 1.0 Hz. Two to three specimens from each film sample with the dimensions of 11.0 mm × 5.0 mm (length × width) were tested.

Results and discussion

Cellulose fraction from birch sawdust after sequential extractions

In the modern concept of biorefinery, sequential extraction of each component from wood allows a distinct fractionation of these components separately for further applications (Liu et al. 2012b). In the present study we have focused on the application of the residual cellulose fraction for NFC preparation. A commercial bleached kraft pulp (BKP), conventionally used for NFC preparation, was applied as a reference. The chemical composition and morphology of the fiber samples used are listed in Table 2. The carboxyl group, –COOH, is an acidic group attached to cellulose chains and is formed mainly by the oxidation of cellulose during pulping and bleaching processes. A certain level of carboxyl groups is also associated with hemicelluloses. In unbleached hardwood pulps, also the unbleached sawdust pulp here, residual lignin and hexuronic acid (HexA) side groups from xylans are the major contributors to carboxyl groups. As reported that nearly 70 % of lignin and HexA can be removed in the first stage of chlorine dioxide bleaching (Loureiro et al. 2010), indicating

Table 2 Fiber morphology, chemical properties, and intrinsic viscosity (η) and degree of polymerization (DP) of the pulps

	Length (mm)	Width (μ m)	Fines content (%)	Carboxylate content (mmol/g)	Hemicellulose (wt%)	η (ml/ g)	DP
Unbleached sawdust pulp	0.61 \pm 0.01	19.2 \pm 0.1	39.4 \pm 0.1	0.158	8.6	705	2,549
Bleached sawdust pulp	0.59 \pm 0.00	19.8 \pm 0.2	42.3 \pm 0.2	0.274	8.3	593	2,104
Reference BKP	0.95 \pm 0.01	22.0 \pm 0.2	10.6 \pm 0.1	0.238	18.6	900	3,346

that the ECF bleached sawdust fiber and the reference BKP shared the similar source of carboxylate content, i.e. mainly arises from the oxidation of cellulose. Hence, the starting materials have a similar carboxylate content and origin. As shown in Table 2 and Table S1, the hemicellulose content of the sawdust pulp was relatively low and remained unchanged after bleaching. This is because most of the hemicelluloses had been extracted by hot-water prior to lignin removal and ECF bleaching. An increase in fines content and decrease in fiber length are probably ascribed to the cutting that appears in sawing and harsh conditions for sequential extraction of hemicelluloses and lignin. The relative short fibers and high fines content make sawdust pulp almost impossible for use by the conventional papermaking industry. However, from another point of view, the short length of the fibers and high fines content are favorable for yielding the nano-scale fibrils desired under milder processes' conditions compared to commercial pulp with normal fiber morphology, therefore requiring lower energy consumption. Thus, this validating the use of bleached sawdust pulp as a starting material for the preparation of NFC.

TEMPO-mediated oxidation of cellulose fibers

In the present study, the residual cellulose in sawdust was converted to NFC suspension with yield of over 85 % depending on the reaction conditions. Higher charged NFC with high yield was obtained compared with the cotton linter NFC reported at the similar conditions (carboxylate content of 0.52 mmol/g and yield of 78 %; Saito and Isogai 2004). The carboxylate content of NFC is a crucial factor which affects the stability of the resultant NFC dispersion. The appearance of a band at 1,730 cm^{-1} in the FTIR spectra (Figure S2) confirms the formation of carboxyl groups in the NFC. The dosage of NaClO and the reaction

time are important parameters for TEMPO-mediated oxidation. In the present study, reaction equilibrium was reached at 4.0 h for the reference BKP and 6.0 h for sawdust fiber at the NaClO dosage of 5 mmol/g fiber respectively, and 9.5 h for both the reference and sawdust fiber at the NaClO dosage of 10 mmol/g fiber. The reason why a longer equilibrium time was needed for sawdust fiber than for the reference at the NaClO dosage of 5 mmol/g could be explained by the lower hemicellulose content of the sawdust fiber. However, even under the same reaction time (4.0 h), the carboxylate content of sawdust fiber (0.956 mmol/g) was higher than that of the reference (0.818 mmol/g). One tentative explanation is the drying history of the pulp; flash drying of the reference in the mill may reduce the accessibility of water swelling and chemical reaction via increasing irreversible hydrogen bonds (hornification effect) and decreasing specific surface areas (Liu et al. 2012a). Moreover, a higher hemicellulose content of the reference (18.6 %) could be another important factor which resulted in lower carboxylate content. This is because 64 % of the hemicelluloses were xylans (Table S1), in which there are no primary hydroxyls available for TEMPO oxidization. However, in accordance with the report of Saito et al. (2007) as shown in Fig. 1, both the never-dried sawdust fiber and the flash-dried reference turned to oxidized cellulose fibrils having a similar carboxylate content of over 1.10 mmol/g, when the equilibrium was reached at a sufficiently high dosage of NaClO (10 mmol/g) and with a longer reaction time (9.5 h). Equilibrium of the reaction can also be confirmed by the trend depicted in Fig. 1, where the carboxylate content of the TEMPO-oxidized cellulose was soaring before equilibrium under each dosage of NaClO and then leveled off. As shown in Fig. 1, the carboxylate content of the products at each equilibrium point was higher than 0.8 mmol/g, which was the lowest limit for the formation of NFC gel at a

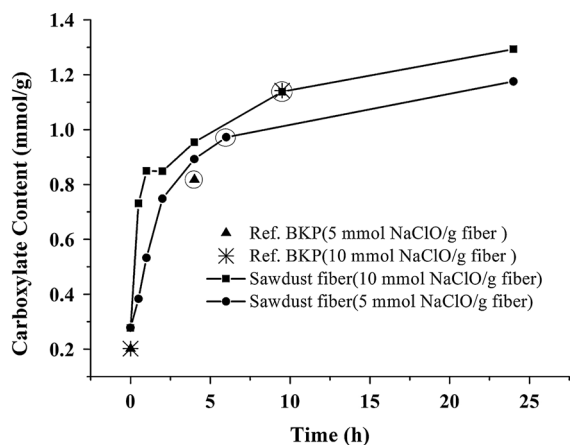


Fig. 1 Carboxylate contents of TEMPO-oxidized celluloses prepared from reference BKP and sawdust fiber using the TEMPO/NaClO/NaBr approach at different NaClO dosages as function of oxidation time. Further analyses of NFC were carried out for the samples in which oxidation reactions reached equilibrium as *circled* in the figure

concentration of 0.5 %. Although extension of the reaction time increased the carboxylate content slightly (Fig. 1), excessive β -elimination of C6 aldehyde groups under alkaline conditions and cleavage of glycosidic bonds by radical species could be detrimental to the polymerization and intrinsic mechanical strength of cellulose, and consequently lowered the potential application (Benhamou et al. 2014; Saito et al. 2009). Herein, further analyses of NFC were carried out for the samples with the oxidation reactions which reached equilibrium, and these samples were circled in Fig. 1 and shown in Table 3. Code names of these NFC suspensions from reference BKP and sawdust fiber with low or high carboxylate content were used as Ref-low, Ref-high, SD-low, and SD-high respectively, the same code names were also applied for their corresponding resultant films.

Optical properties of NFC suspension and films

Visual observation of the NFC suspension in Fig. 2 clearly revealed the significant effect of carboxylate content on the dispersion of NFC. A totally transparent and stabilized dispersion of oxidized cellulose was obtained after the carboxylate content of NFC approaching to 1.16 mmol/g in the present study. The strong electrostatic repulsion allowed the cellulose nanofibrils to be well-dispersed. However, some visible fibrils in the NFC resulted in translucent optical behavior when the carboxylate contents were lower than 1.16 mmol/g.

Transmission electron microscopy (TEM) images of NFC suspensions of the reference and the sawdust fibers are presented in Fig. 3. The individual cellulose fibrils of the reference, as shown in Fig. 3a, had a size of 5 nm in width and hundreds of nanometers to microns in length. Dimensions of the individual cellulose fibrils from the sawdust fibers were also ca. 5 nm in width and hundreds of nanometers in length (Fig. 3b, c). Thus the fibrils were thinner in diameter compared with the reported nanofibers with a width of 15 nm obtained by grinding treatment of wood powder (Abe et al., 2007). Besides, as shown in Fig. 3b and also reported by other researchers (Dalmás et al. 2007; Saito et al. 2007), partially, NFC fibrils that had a lower carboxylate content (Fig. 3b, SD-low, carboxylate content of 0.92 mmol/g) formed lateral aggregates and arranged themselves in bundles of ca. 20 nm in width. The lower original fiber length and DP (Table 2) of sawdust pulp and the bleaching of the sawdust KP could also be the reason for the relative lower length of the NFC from sawdust fibers (Fukuzumi et al. 2012).

NFC suspensions and films with higher carboxylate content allowed higher light transmittance (Figure

Table 3 TEMPO oxidation equilibrium conditions of reference and sawdust fiber

Sample	NaClO dosage (mmol/g fiber)	Oxidation time (h)	Carboxylate content (mmol/g)	η (ml/g)	DP
Reference BKP (Ref-low)	5	4.0	0.85 ± 0.03	—	—
Reference BKP (Ref-high)	10	9.5	1.17 ± 0.06	168	521
Sawdust fiber (SD-low)	5	6.0	0.92 ± 0.04	—	—
Sawdust fiber (SD-high)	10	9.5	1.16 ± 0.03	153	467

Low and high correspond to the carboxylate contents of the reference BKP (Ref) and sawdust fiber (SD). These code names will be used in the following context

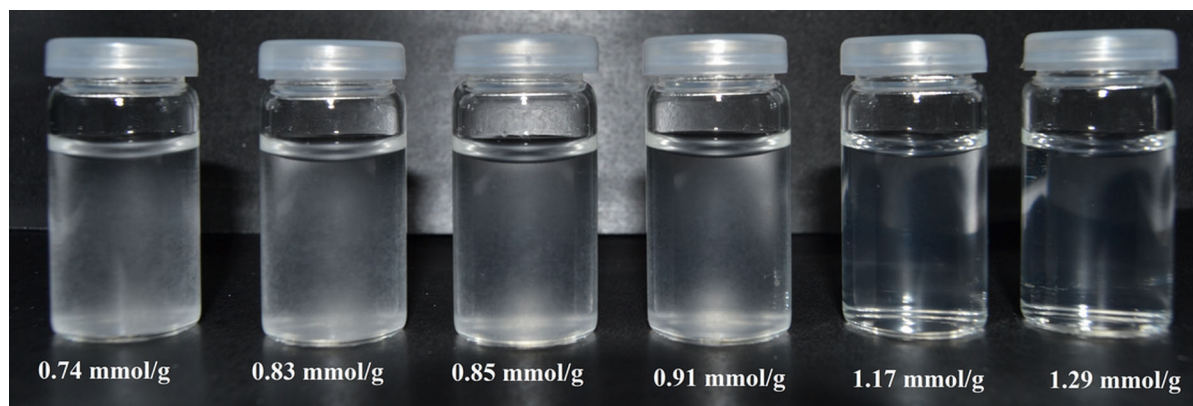


Fig. 2 Photographs of the NFC suspension (0.1 %) of TEMPO-oxidized sawdust fiber with different carboxylate contents. The carboxylate content of each sample is illustrated under each sample

S1). However, an intriguing phenomenon observed is that the NFC from the reference always showed higher transmittance when two samples had close carboxylate contents. Here, we suppose that the morphology of the NFC, as discussed with the TEM images, could be the main reason for this unexpected optical behavior. The NFC prepared from the reference possessed smaller width and higher values in length, i.e., a higher aspect ratio. The Rayleigh scattering law reveals that particle with a smaller diameter, the width of the NFC here, scatters less light and the transmittance increases with decreasing particle size.

Surface morphology of NFC films

The films were viewed with microscopes to obtain information about their morphology. NFC can be visualized by polarizing optical microscopy (P-OM) as bright particles in (Fig. 4b, d, f). This is due to its characteristic of orientating polarized light, which indicates crystalline structures (Mikkonen et al. 2011, 2012a; Cranston and Gray 2008). As shown in Fig. 4a–d, no significant difference can be observed from both optical microscopy (OM) and P-OM images of films from the NFC of Ref-low and SD-low. Moreover, all consisted of visible compact fibrous rod structures dispersed randomly in all directions in the OM images and partially blocked bright spots in the P-OM images. The black fibrils in the OM images of these lower charged samples, on the other hand, indicated that the dispersion of fibrils by the electrostatic repulsion of carboxylate group was insufficient.

However, the OM images of NFC films from sample SD-high (Fig. 4e) were much more even and the sparse visible fibers were thinner than those in samples Ref-low (Fig. 4a) and SD-low (Fig. 4c). The packed bright spots in the P-OM image in Fig. 4f were uniform in size and evenly distributed, suggesting a well dispersion of the crystalline cellulose. The O'Connor's infrared crystallinity indexes (O'KI) data from the FTIR support this observation (Figure S2, Table S2). This observation of OM and P-OM of films was in accordance with the results of the TEM images analysis.

Moreover, as shown in Fig. 4g, entangled nanofibrils network without any trace of visible fragment of fibers can also be observed in the scanning electron microscopy (SEM) image of the NFC film prepared from sawdust fiber (SD-high).

Mechanical properties of NFC films

Static mechanical properties of the films

The tensile properties shown in Fig. 5a and Table 4 were determined for films from NFC samples in which oxidation reactions reached equilibrium, as listed in Table 3.

The Young's modulus of the films were calculated by extrapolation at the initial quasi-linear portion of the curves and listed the results in Table 4 as averages of ten specimens (Nechwatal et al. 2003). There was no significant difference in the Young's modulus of the films prepared from sawdust fibers and the

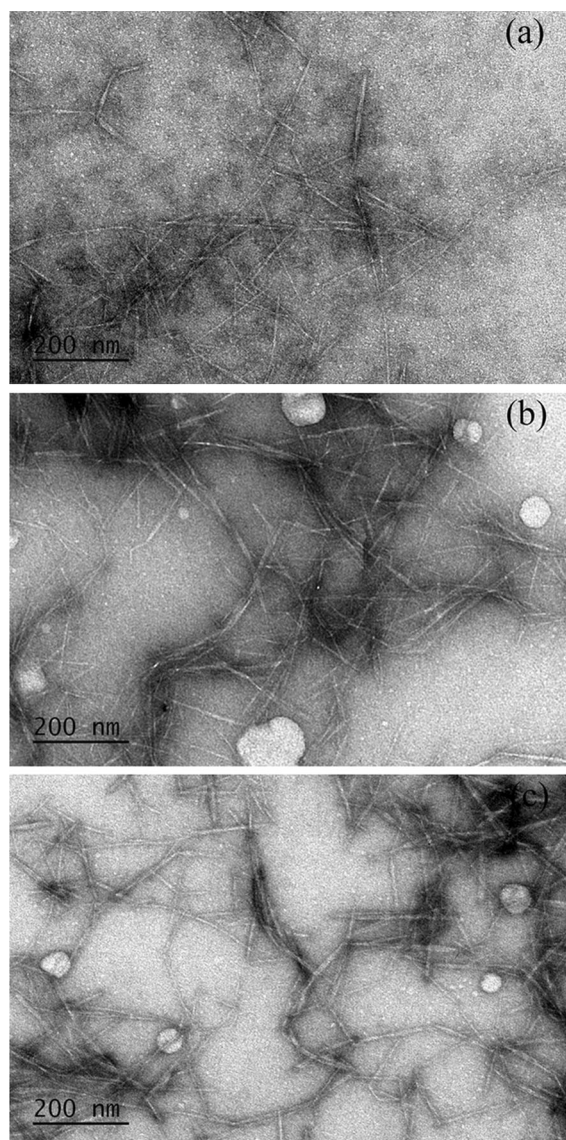


Fig. 3 TEM images of NFC suspensions prepared from **a** Ref-high, **b** sawdust fiber SD-low, and **c** sawdust fiber SD-high. *NB:* Equilibrium conditions and the code names of the samples are shown in Table 3 (same as below)

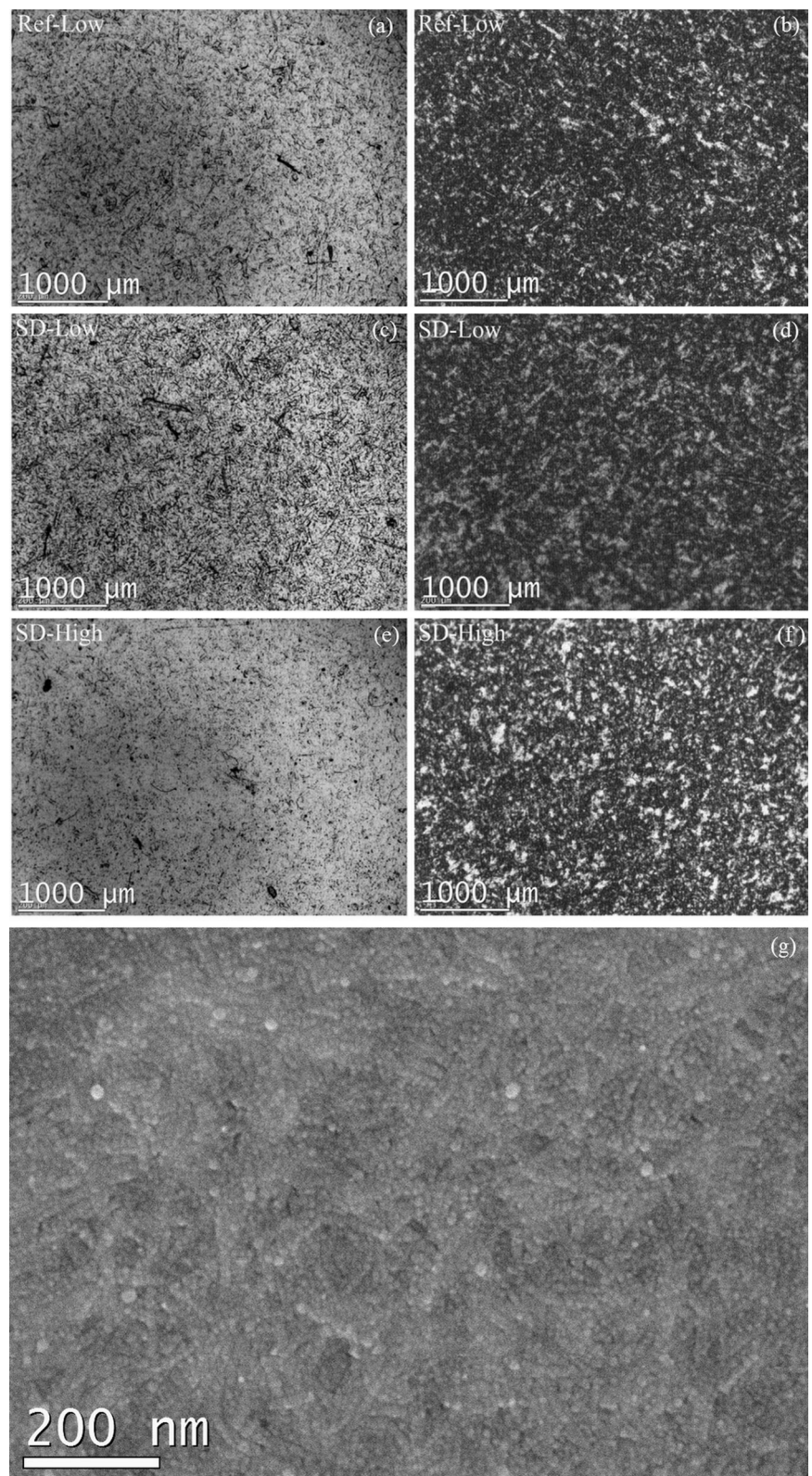
reference; however, tensile strength and elongation of the films prepared from sawdust fibers showed higher values. These results were close to or even better than some of the reported NFC films (Klemm et al. 2011). As can be seen from the data of the reference, extended oxidation time and a higher dosage of NaClO could be detrimental to the polymerization and intrinsic mechanical strength of cellulose and consequently lowered the mechanical strength of the films, while the

elongation of the films from sawdust fibers slightly increased. On the contrary, relatively harsh reaction conditions enhanced the mechanical strength of NFC films of sawdust fibers. Here, we hypothesize that the even dispersion of NFC particles in NFC films obtained from sawdust fiber can offer a better fiber–fiber interface interaction which exhibited in higher elongation and tensile strength than that of reference sample. Also, it has been emphasized by Liu and Berglund (2012) that a homogeneous dispersion is beneficial for forming a film with a high modulus, significant strength and toughness. Fewer laterals, aggregates and bundles (Fig. 3c) of NFC, and increased homogeneous NFC particles (Fig. 4e) of the NFC film prepared in a radical condition could form a better fiber–fiber interface that contributes to efficient stress transfer between NFC particles. Besides, the relatively smaller size of NFC provides a larger available surface area which contributes to a larger number of hydrogen bonds and thus stronger materials. Notably, the mechanical behavior (especially elongation) of the films prepared from sawdust fibers was better than that of the reference.

Dynamic mechanical properties of NFC films

The storage modulus of NFC films as a function of temperature is shown in Fig. 5b. NFC films prepared from sawdust fibers (SD-low and SD-high) showed higher stiffness than that from the reference (Ref-low and Ref-high). The influence of carboxylate content (SD-low, 0.92 mmol/g; SD-high, 1.16 mmol/g) of the NFC on the storage modulus of films has exhibited a significant difference for sawdust fibers due to inter-molecular forces, i.e. hydrogen bonding of carboxyl groups. However, for NFC films from the reference, the storage modulus was rather similar regardless of the carboxylate content of the NFC (Ref-low, 0.85 mmol/g; Ref-high, 1.17 mmol/g). This indicates that the films from the reference BKP with different carboxylate contents responded similarly to the low forces applied to the films at the elastic range. The storage modulus of the films prepared from sawdust fibers (SD-low and SD-high) showed higher values than for the reference (Ref-low and Ref-high) under the whole temperature range, even for the samples of Ref-high and SD-high which were prepared at the same conditions and had similar carboxylate contents. Other factors such as the distribution of crystalline

Fig. 4 Optical (*top left column, a, c and e*) and polarizing optical (*top right column, b, d and f*) microscopy images of NFC films prepared from the reference sample Ref-low and sawdust fibers sample SD-low and SD-high. SEM images (*below, g*) of the NFC film surface prepared from sawdust fiber sample SD-high



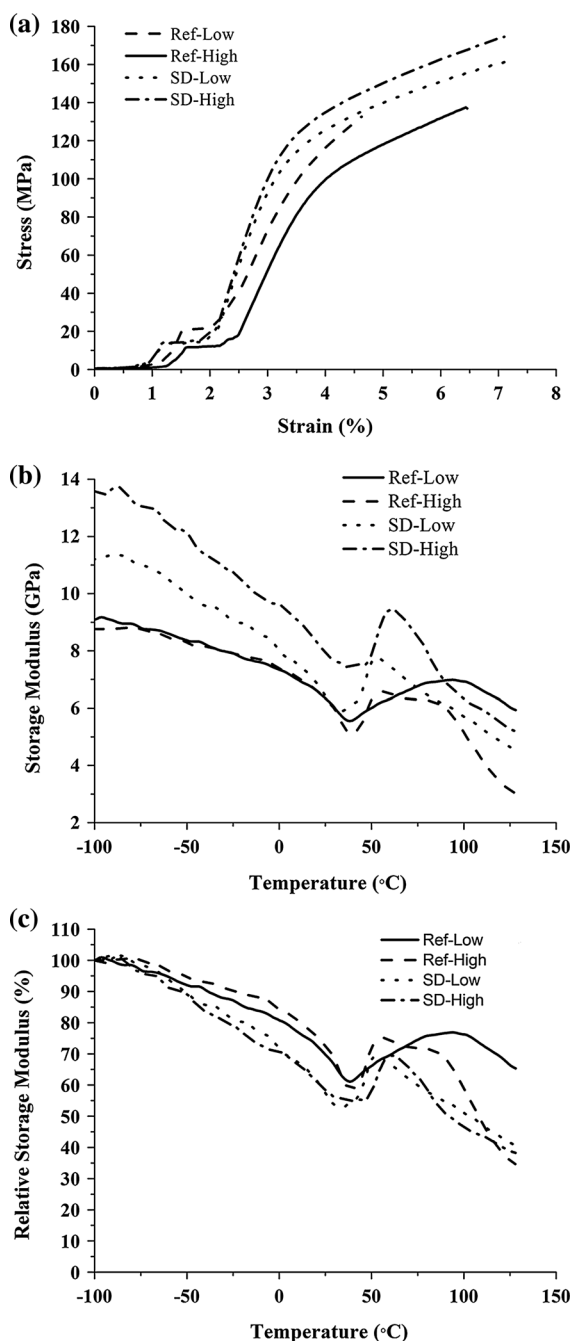


Fig. 5 Selected representative stress–strain (a), storage modulus (b) and relative storage modulus (c) curves of NFC films prepared from reference samples (Ref-low and Ref-high), and sawdust fiber samples (SD-low and SD-high)

cellulose and the crystallinity (O'Connor's infrared crystallinity indexes, Table S2) might also affect the response of elastic deformation. Another noticeable

Table 4 Static mechanical properties of NFC films

Sample	Young's modulus (GPa)	Tensile strength (MPa)	Elongation (%)	Density (g/cm ³)
Ref-low	6.4 ± 0.5	159.3 ± 9.3	5.2 ± 0.7	1.03
Ref-high	5.9 ± 0.5	151.2 ± 13.2	6.0 ± 0.8	0.99
SD-low	6.0 ± 0.5	161.5 ± 5.0	7.4 ± 0.5	0.99
SD-high	6.4 ± 0.5	171.6 ± 9.9	7.6 ± 0.5	1.03

phenomenon is that all the curves showed a peak at 50–55 °C, which could indicate stiffening of the films due to water evaporation (the samples were conditioned at 50 % RH before measurement). Loss of moisture induced material plasticization, which could increase the formation of hydrogen bonds between cellulose fibrils and consequently increase the storage modulus of the films. This stiffness effect was retained in a wider temperature range for the reference. The effect of moisture evaporation on the dynamic mechanical properties of polysaccharide matrices, as reported also by Mikkonen et al. (2012a), supports this proposition.

The relative storage modulus, shown in Fig. 5c, depicts the ratio of the modulus of the films at a given temperature to its initial modulus, revealing the softening behavior of the films with the increase in temperature (Mikkonen et al. 2012b). The trend of the curves was similar to that of the absolute storage modulus in Fig. 5b, but the films from sawdust fibers showed a lower relative storage modulus than that for the reference in the whole temperature range. The relative storage modulus decreased by 34.7 % for the sample of Ref-low and by 59.5 % for the sample of SD-low at the same highest temperature. This suggests that the film from sawdust fibers restored less energy of the low forces applied to the films at the elastic range. In other words, it softened at a lower temperature than the films from the reference.

Conclusion

This study has demonstrated the feasibility of producing NFC and its films with high mechanical properties from a wood waste—birch sawdust for the first time by a process incorporated into a novel biorefinery platform. The NFC, with a dimension of ca. 5 nm in width

and hundreds of nanometers in length, and its resulting films prepared from sawdust BKP show comparable or even better mechanical properties than those from the reference BKP at the same condition. Carboxylate content and geometric morphology play an important role in the dispersion of the NFC suspension and transmittance of light. The NFC suspension and its films may find potential applications in advanced materials as matrix or reinforcement additives.

Acknowledgments The authors would like to acknowledge the financial support of the China Scholarship Council. We thank Dr. Jan Gustafsson for access to the FiberLab instrument. Prof. Maija Tenkanen at the University of Helsinki is gratefully acknowledged for valuable discussions. Chunlin Xu also thanks the Knut and Alice Wallenberg Foundation for financial support via the KTH Wallenberg Wood Science Center. This work was also part of the activities at the Åbo Akademi Process Chemistry Centre.

References

- Abdul Khalil HPS, Bhat AH, Ireana Yusra AF (2012) Green composites from sustainable cellulose nanofibrils: a review. *Carbohydr Polym* 87(2):963–979
- Abe K, Iwamoto S, Yano H (2007) Obtaining cellulose nanofibers with a uniform width of 15 nm from wood. *Biomacromolecules* 8(10):3276–3278
- Araki J, Wada M, Kuga S (2001) Steric stabilization of a cellulose microcrystal suspension by poly(ethylene glycol) grafting. *Langmuir* 17(1):21–27
- Benhamou K, Dufresne A, Magnin A, Mortha G, Kaddami H (2014) Control of size and viscoelastic properties of nanofibrillated cellulose from palm tree by varying the TEMPO-mediated oxidation time. *Carbohydr Polym* 99:74–83
- Blot WJ (1997) Wood dust and nasal cancer risk. A review of the evidence from North America. *J Occup Environ Med* 39(2):148–156
- Borrega M, Tolonen LK, Bardot F, Testova L, Sixta H (2012) Potential of hot water extraction of birch wood to produce high-purity dissolving pulp after alkaline pulping. *Bioresour Technol* 135:665–671
- Cranston ED, Gray DG (2008) Birefringence in spin-coated films containing cellulose nanocrystals. *Colloids Surf A* 325(1–2):44–51
- Dalmas F, Cavallé JY, Gauthier C, Chazeau L, Dendievel R (2007) Viscoelastic behavior and electrical properties of flexible nanofiber filled polymer nanocomposites. Influence of processing conditions. *Compos Sci Technol* 67(5):829–839
- Demers PA, Boffetta P, Kogevinas M, Blair A, Miller BA, Robinson CF, Roscoe RJ, Winter PD, Colin D, Matos E, Vainio H (1995) Pooled reanalysis of cancer mortality among five cohorts of workers in wood-related industries. *Scand J Work Environ Health* 21(3):179–190
- Ebringerová A, Hromádková Z, Hříbalová V, Xu CL, Holmbom B, Sundberg A, Willför S (2008) Norway spruce galactoglucomannans exhibiting immunomodulating and radical-scavenging activities. *Int J Biol Macromol* 42(1):1–5
- Eurostat (2013) <http://epp.eurostat.ec.europa.eu/portal/page/portal/forestry/introduction>. Accessed Jan 2013
- Evans R, Wallis AFA (1989) Cellulose molecular weight determined by viscosity. *J Appl Polym Sci* 37:2331–2340
- FitzPatrick M, Champagne P, Cunningham MF, Whitney RA (2010) A biorefinery processing perspective: treatment of lignocellulosic materials for the production of value-added products. *Bioresour Technol* 101(23):8915–8922
- Fukuzumi H, Saito T, Isogai A (2012) Influence of TEMPO-oxidized cellulose nanofibril length on film properties. *Carbohydr Polym* 93(1):172–177
- Klemm D, Kramer F, Moritz S, Lindstrom T, Ankerfors M, Gray D, Dorris A (2011) Nanocelluloses: a new family of nature-based materials. *Angew Chem Int Ed* 50(24):5438–5466
- Liu AD, Berglund LA (2012) Clay nanopaper composites of nacre-like structure based on montmorillonite and cellulose nanofibers—improvements due to chitosan addition. *Carbohydr Polym* 87(1):53–60
- Liu J, Hu HR, Xu JF, Wen YB (2012a) Optimizing enzymatic pretreatment of recycled fiber to improve its draining ability using response surface methodology. *BioResources* 7(2):2121–2140
- Liu SJ, Lu HF, Hu RF, Shupe A, Lin L, Liang B (2012b) A sustainable woody biomass biorefinery. *Biotechnol Adv* 30(4):785–810
- Loureiro PEG, Domingues EF, Evtuguin DV, Graça Videira Sousa Carvalho M (2010) ECF bleaching with a final hydrogen peroxide stage: impact on the chemical composition of eucalyptus globulus kraft pulps. *BioResources* 5(4):2567–2580
- Mikkonen KS, Stevanic J, Joly C, Dole P, Pirkkalainen K, Serimaa R, Salmén L, Tenkanen M (2011) Composite films from spruce galactoglucomannans with microfibrillated spruce wood cellulose. *Cellulose* 18(3):713–726
- Mikkonen KS, Pitkänen L, Liljeström V, Bergström EM, Serimaa R, Salmén L, Tenkanen M (2012a) Arabinoxylan structure affects the reinforcement of films by microfibrillated cellulose. *Cellulose* 19(2):467–480
- Mikkonen KS, Heikkilä M, Willför S, Tenkanen M (2012b) Films from glyoxal-crosslinked spruce galactoglucomannans plasticized with sorbitol. *Int J Polym Sci*. doi:10.1155/2012/482810
- Nechwatal A, Mieck KP, Reusmann T (2003) Developments in the characterization of natural fibre properties and in the use of natural fibres for composites. *Compos Sci Technol* 63(9):1273–1279
- Ohara H (2003) Biorefinery. *Appl Microbiol Biotechnol* 62(5–6):474–477
- Okita Y, Saito T, Isogai A (2009) TEMPO-mediated oxidation of softwood thermomechanical pulp. *Holzforschung* 63(5):529–535
- Saito T, Isogai A (2004) TEMPO-medicated oxidation of native cellulose. The effect of oxidation conditions on chemical

- and crystal structures of the water-insoluble fractions. *Biomacromolecules* 5(5):1983–1989
- Saito T, Kimura S, Nishiyama Y, Isogai A (2007) Cellulose nanofibers prepared by TEMPO-mediated oxidation of native cellulose. *Biomacromolecules* 8(8):2485–2491
- Saito T, Hirota M, Tamura N, Kimura S, Fukuzumi H, Heux L, Isogai A (2009) Individualization of nanosized plant cellulose fibrils by direct surface carboxylation using TEMPO catalyst under neutral conditions. *Biomacromolecules* 10(7):1992–1996
- Siqueira G, Bras J, Dufresne A (2010) Cellulosic bionanocomposites: a review of preparation, properties and applications. *Polymers* 2(4):728–765
- Song T, Pranovich A, Holmbom B (2011) Effects of pH control with phthalate buffers on hot-water extraction of hemicelluloses from spruce wood. *Bioresour Technol* 102(22):10518–10523
- Tatrai E, Adamis Z, Bohm U, Meretey K, Ungvary G (1995) Role of cellulose in wood dust-induced fibrosing alveolo-bronchiolitis in rat. *J Appl Toxicol* 15(1):45–48
- Weber S, Kullman G, Petsonk E, Jones WG, Olenchock S, Sorenson W, Parker J, Marcelo-Baciu R, Frazer D, Castanova V (1993) Organic dust exposures from compost handling: case presentation and respiratory exposure assessment. *Am J Ind Med* 24(4):365–374
- Zakzeski J, Bruijninx PCA, Jongerius AL, Weckhuysen BM (2010) The catalytic valorization of lignin for the production of renewable chemicals. *Chem Rev* 110(6):3552–3599